Journal of Thermal Analysis and Calorimetry (2020) 140:625–636
https://doi.org/10.1007/s10973-019-08897-z

Effect of aluminum diethylphosphinate on flame retardant and thermal properties of rigid polyurethane foam composites

Gang Tang[1,2] · Lin Zhou[2] · Ping Zhang[2] · Zhongqiang Han[3] · Depeng Chen[1] · Xiuyu Liu[1] · Zijian Zhou[1]

Received: 7 April 2019 / Accepted: 8 October 2019 / Published online: 30 October 2019

Abstract

Rigid polyurethane foam/aluminum diethylphosphinate (RUPF/ADP) composites were prepared by one-step water-blown method. Furthermore, scanning electron microscope (SEM), thermal conductivity meter, thermogravimetric analysis (TGA), limiting oxygen index, Underwriters Laboratories vertical burning test (UL-94) and microsacle combustion calorimetry were applied to investigate thermal conductivity, thermal stability, flame retardancy and combustion behavior of RPUF/ADP composites. Thermogravimetric analysis–Fourier transform infrared spectroscopy (TG–FTIR) was introduced to investigate gaseous products in degradation process of RPUF/ADP composites, while SEM and X-ray photoelectron spectroscopy were used to research char residue of the composites. It was confirmed that RPUF/ADP composites presented well cell structure with density of 53.1–59.0 kg m^{-3} and thermal conductivity of 0.0425–0.0468 W m^{-1} K^{-1}, indicating excellent insulation performance of the composites. Flame retardant test showed that ADP significantly enhanced flame retardancy of RPUF/ADP composites, RPUF/ADP30 passed UL-94 V-1 rating with LOI of 23.0 vol%. MCC test showed that ADP could significantly decrease peak of heat release rate (PHPR) of RPUF/ADP composites. PHPR value of RPUF/ADP20 was decreased to 158 W g^{-1}, which was 21.8% reduced compared with that of pure RPUF. TG–FTIR test revealed that the addition of ADP promoted the release of CO_2, hydrocarbons and isocyanate compound in first-step degradation of RPUF matrix while inhibited the release of CO in second step degradation. Char residue analysis showed that the addition of ADP promoted polyurethane molecular chain to form aromatic and aromatic heterocyclic structure, enhancing strength and compactness of the char. This work associated a gas–solid flame retardancy mechanism with the incorporation of ADP, which presented an effective strategy for preparation of flame retardant RPUF composites.

Keywords Rigid polyurethane foam · Flame retardant · Composites · Thermal properties

Introduction

Polyurethane (PU), as a high performance polymer, was used as elastomer, foam, coating, fiber, plastic et al in many fields [1–4].In these materials, rigid polyurethane foam (RPUF), owning to its excellent thermal insulation performance and good mechanical properties, was widely applied as thermal insulating materials in many fields, especially in building construction [5–8]. However, disadvantage of flammability for RPUF significantly restricted its wide application. Thus, a great deal of efforts was conducted to improve the flame retardancy of RPUF composites [9–12]. Generally, flame retardancy of RPUF can be enhanced by incorporation reactive or additive flame retardant [13]. Usually, reactive flame retardant RPUF was prepared by involving phosphorus-containing diols and polyols [14, 15]. However, this strategy was restricted for high coat.

✉ Gang Tang
tanggang@ahut.edu.cn

✉ Ping Zhang
pingzhang@swust.edu.cn

[1] School of Architecture and Civil Engineering, Anhui University of Technology, 59 Hudong Road, Ma'anshan 243002, Anhui, China

[2] State Key Laboratory of Environment-friendly Energy Materials & School of Materials Science and Engineering, Southwest University of Science and Technology, Mianyang 621010, Sichuan, China

[3] State Key Laboratory of Special Functional Waterproof Materials, Beijing Oriental Yuhong Waterproof Technology Co., Ltd., Beijing 101309, China

The most commonly method to improve flame retardancy of RPUF was add flame retardants into RPUF matrix. Some traditional flame retardants, such as expandable graphite, ammonium polyphosphate and red phosphorus were applied to enhance flame retardancy of RPUF [16, 17]. Li et al. prepared β-Cyclodextrin modified ammonium polyphosphate (β-APP) and incorporated it into RPUF to improve thermal stability and flame retardancy. RPUF composites with 25 mass% β-APP incorporation presented 67.3% reduced of flame spread speeding compared with pure RPUF and extinguish time decreased to 2.1 s [16]. Wang et al. prepared aluminum hydroxide encapsulated expandable graphite (EG@ATH) and introduced it into RPUF composites, which presented LOI value of 29.6 vol% with 11.5 mass% of EG@ATH loading [12]. Cao et al. [17] prepared coated red phosphorus (MRP) to improve fire retardancy and smoke suppression of RPUF composites and found that 80 php (parts per hundreds of polyol) of MRP loading increased the LOI value of RPUF composites to high than 25%.

Aluminum diethylphosphinate (ADP), as a novel halogen-free flame retardant, can be good candidate for preparation of halogen-free flame retardant composites as well as metal hydroxide, layered double hydroxides, carbon nanotubes, montmorillonite, copper phenylphosphate et al [18–23]. For its high fire retarding performance, ADP was introduced to fabricate a series of flame retarded polymer composites [24–27]. Zhan et al. [24] reported that polyamide 6, 6 (PA 66) composites passed UL-94 V0 rating (1.6 mm) with LOI of 33.4 vol% when ADP loading was 14 mass%. Wang et al. investigated the synergistic flame retardant effect of aluminum diethylphosphinate and aluminum hydroxide in unsaturated polyester resin (UPR) composites. It was revealed that UPR composites presented LOI of 30.0 vol% with UL-94 V0 rating when 15 mass% of ADP and 10 mass% of ATH were added [25]. Gu et al. reported the application of ADP in epoxy resin (EP) composites, and it was found that EP composites reached V0 rating in UL-94 test and LOI of 37.2 vol% with of relatively low ADP loading of 8.4 mass% [26]. Kaya et al. [27] investigated different nanoparticles on thermal stability of polylactide/aluminum diethyl phosphinate composites and found that the combination of montmorillonite and aluminum diethylphosphinate could significantly enhance thermal characteristics of PLA composites.

As far as we know, few research reported have focus on flame retarded rigid polyurethane foam with ADP. Thus, ADP was introduced to prepare flame retardant RPUF composites in this work. The thermal conductivity, thermal stability, flame retardancy and combusition properties of RPUF composites were investigated by thermal conductivity meter, thermal gravimetric analysis (TGA), microscale combustion calorimetry (MCC), limiting oxygen index (LOI) and UL-94 vertical burning test. The gaseous pyrolysis products of the composites were investigated by TG–FTIR. In addition, X-ray photoelectron spectroscopy (XPS) and scanning electron microscope (SEM) were used to research the char residue of the composites.

Experimental

Materials

LY-4110 (viscosity: 2500 mPa s, hydroxyl number: 430 mg KOH/g), Triethylenediamine (A33, 33%) and silicone surfactant (AK8805) were provided by Jiangsu Luyuan New Materials Co., Ltd, China. Polyaryl polymethylene isocyanate (PAPI) was provided by Wanhua Chemical Group Co., Ltd, China. Dibutyltin dilaurate (LC) was purchased from Air Products and Chemicals, Inc. Triethanolamine (TEOA) was purchased from Sinopharm Chemical Reagent Co., Ltd, China. Distilled water used as a chemical blowing agent was made in our laboratory. Aluminum diethylphosphinate (ADP) was purchased from Qingdao Fuslin Chemical Technology Co., Ltd.

Preparation of rigid polyurethane foam composites

RPUF composites were prepared by one-shot and free-rise method, and the formulation of the composites is shown in Table 1. All of the raw materials except PAPI were mixed well in a 1000 mL plastic beaker by high speed mechanical stirrer. PAPI was poured into the mixture with vigorous stirring for 10 s and quickly added into a mold (300 mm × 200 mm × 60 mm). Subsequently, the resultant foam was allowed to cure for 5 h at 80 °C to complete the polymerization reaction. The foams were cut into suitable size for further characteristics. The detailed formulation for the samples is shown in Table 1.

Measurement and characterization

Scanning electron microscopy (SEM, JSM-6490LV, JEOL Ltd, Japan) was applied to observe the cellular structure of the foams with accelerating voltage of 20 kV. Prior to observation, the sample surface was coated with a thin conductive layer.

Thermal conductivity was measured according to GB/T 10297-2015 by thermal conductivity meter (TC3000E, Xiaxi Electronic Technology Co., Ltd, China) with sample size of 30 mm × 30 mm × 25 mm. Five parallels for each sample were tested and the average value was reported.

The apparent density of RPUF composites was measured according to ISO 845-2006, in which the size of the sample was no less than 100 cm^3. Also, five samples were tested to obtain average values.

Thermogravimetric analysis (TGA) was performed by Q5000IR (TA Instruments, USA) thermo-analyzer

Table 1 Formulation of RPUF and RPUF/ADP composites

Sample	LY4110/php[a]	PM-200/php	LC/php	AK-8805/php	A33/php	Water/php	TEA/php	ADP/php
RPUF	100	150	0.5	2	1	2	3	0
RPUF/ADP5	100	150	0.5	2	1	2	3	5
RPUF/ADP10	100	150	0.5	2	1	2	3	10
RPUF/ADP15	100	150	0.5	2	1	2	3	15
RPUF/ADP20	100	150	0.5	2	1	2	3	20
RPUF/ADP25	100	150	0.5	2	1	2	3	25
RPUF/ADP30	100	150	0.5	2	1	2	3	30

[a]Parts per hundreds of polyol

instrument. 5–10 mg sample was heated to 800 °C with a linear heating rate of 20 °C min^{-1} under nitrogen flow of 70 mL min^{-1}.

Limiting oxygen index (LOI) value was determined at room temperature by JF-3 oxygen index instrument (Jiangning Analysis Instrument Co., Ltd, China) according to ASTM D2863-97. The size of the sample was 127 mm × 10 mm × 10 mm.

The vertical burning test was measured by CZF-3 instrument (Jiangning Analysis Instrument Co., Ltd, China) according to ASTM D3801-96. The dimension of the specimen was 127 mm × 13 mm × 10 mm.

Combustion properties of the sample were characterized by microsacle combustion calorimetry (Govmark, USA) according to ASTM D7309-7. 4–6 mg sample was heated from 100 to 650 °C at 1 °C s^{-1} in a stream of nitrogen flow of 80 mL min^{-1}. The volatile anaerobic thermal degradation products in nitrogen gas stream mixed with 20 mL min^{-1} stream of pure oxygen gas prior to entering a 900 °C combustion furnace. The MCC data obtained were reproducible to about 3%.

Char residues of the sample were obtained by calcining the sample in 600 °C for 10 min. The morphology of the char residue was investigated by scanning electron microscopy (JSM-6490LV, JEOL Ltd, Japan) with accelerating voltage of 20 kV. The specimens were sputter-coated with a conductive layer.

Thermogravimetric analysis–Fourier Transform Infrared Spectrometer (TG–FTIR) was conducted by using Q5000IR (TA Instruments, USA) thermo-analyzer instrument which linked to Nicolet 6700 FTIR spectrophotometer (Thermo Scientific Nicolet, USA). About 5–10 mg of the sample was put in an alumina crucible and heated from 30 to 700 °C. The heating rate was 20 °C min^{-1} in nitrogen atmosphere with flow rate of 70 mL min^{-1}.

X-ray photoelectron spectroscopy (XPS) with a VG Escalab Mark II spectrometer (Thermo-VG Scientific Ltd. USA) using Al Ka excitation radiation ($h\nu = 1253.6$ eV) was used to analyze the char residue of the sample.

Result and discussion

Apparent density

Density was an important parameter that influenced mechanical, thermal conductivity, morphology and water absorption of RPUF composites [28, 29]. Generally, the foam density depended on the foaming agent loading. In this work, the chemical foaming agent and other raw materials (except ADP) were kept constant. Thus, the density value of the composites was depended on ADP loading. Table 2 presents the apparent density values of RPUF and RPUF composites with different ADP loadings. It can be found that RPUF presented density of 58.8 kg m^{-3}. When 5 php ADP was added, RPUF/ADP5 presented density of 55.3 kg m^{-3}. The further increase in ADP loading resulted in further decrease in density of RPUF/ADP composites. When ADP loading was increased to 20–30 php, PRUF/ADP composites presented density of 58.0–59.0 kg m^{-3}. Generally, ADP loading showed limited effect on density of RPUF/ADP composites.

Thermal conductivity

Table 2 also showed the effect of ADP loading on thermal conductivity of RPUF/ADP composites. It can be found that PRUF

Table 2 Apparent density and thermal conductivity of RPUF and RPUF/ADP composites

Sample	ρ/kg m^{-3}	λ/W m^{-1} k^{-1}
RPUF	58.8	0.0392
RPUF/ADP5	55.3	0.0425
RPUF/ADP10	53.4	0.0427
RPUF/ADP15	53.1	0.0430
RPUF/ADP20	59.0	0.0443
RPUF/ADP25	58.1	0.0463
RPUF/ADP30	58.0	0.0468

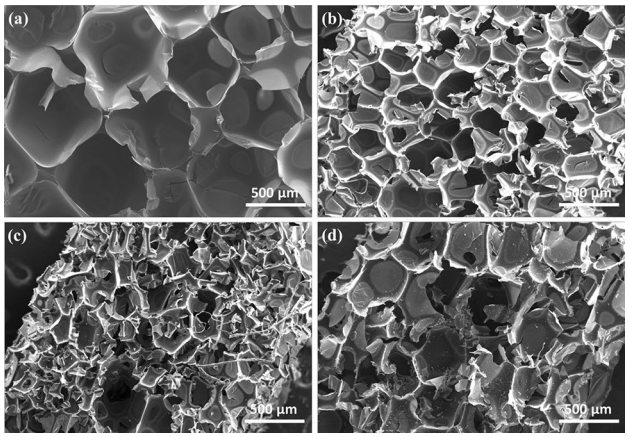

Fig. 1 SEM images of RPUF and RPUF/ADP composites: **a** RPUF; **b** RPUF/ADP10; **c** RPUF/ADP20; **d** RPUF/ADP30

possessed low thermal conductivity of 0.0392 W m^{-1} K^{-1}. When 5 php ADP was added, RPUF/ADP5 presented higher thermal conductivity of 0.0425 W m^{-1} K^{-1}, this may come from that ADP particles had higher thermal conductivity compared with that of RPUF matrix. The further increase in ADP loading resulted in slight increase in thermal conductivity of RPUF/ADP composites. When 30 php ADP was added, RPUF/ADP30 presented thermal conductivity of 0.0468 W m^{-1} K^{-1}, with an increase of 19.4% compared with pure RPUF. Generally, RPUF/ADP composites presented relatively low thermal conductivity.

Morphology

The microstructure of PRUF and RPUF/ADP composites was observed by SEM. As shown in Fig. 1, pure RPUF presented uniform closed polyhedron structures with average cell size of 600 μm. When 10 php ADP was loaded, RPUF/ADP10 showed inhomogeneous microstructure with decreased cell size of 300–400 μm, this may come from that ADP particles acted as nucleating agent which enhanced heterogeneous cell nucleation by decreasing free energy barrier [30]. However, high loading of ADP resulted in rupture of cell structure in RPUF/ADP20 and RPUF/ADP30, suggesting poor compatibility between ADP particles and RPUF matrix.

Flame retardant property

Limiting oxygen index and UL-94 vertical burning test were applied to investigate the effect of ADP loading on flame retardant of RPUF/ADP composites. As shown in Table 3, neat RPUF presented LOI value of 18.8 vol% with NR rating in UL-94 test, indicating poor flame retardancy of RPUF. When 5 php of ADP added into RPUF, RPUF/ADP5 showed

Table 3 LOI and UL-94 test results of RPUF and RPUF/ADP composites

Sample	LOI/vol%	UL-94. 3.2 mm bar		
		t_1/t_2^a/s	Dripping	Rating
RPUF	18.8	28.2/0	N	NR[b]
RPUF/ADP5	21.3	20.3/0	N	V-1
RPUF/ADP10	22.0	18.4/0	N	V-1
RPUF/ADP15	22.3	17.1/0	N	V-1
RPUF/ADP20	22.4	16.7/0	N	V-1
RPUF/ADP25	22.6	16.9/0	N	V-1
RPUF/ADP30	23.0	16.4/0	N	V-1

[a] t_1 and t_2, average combustion times after the first and the second applications of the flame

[b] *NR* not rated

increased LOI value of 21.3 vol% with V-1 rating in UL-94 test. RPUF/ADP composites presented increased LOI values and decreased t_1 values with the further increase in ADP loading. When ADP loading was increased to 30 php, RPUF/ADP30 possessed LOI value of 23.0 vol%. The significant enhancement of fire resistance for RPUF/ADP composites was caused by followed reasons: Firstly, the gas degradation products of ADP (such as oligomers of phosphinates, diethylphosphinic acid) further decomposed to form P· and PO· radicals, which can terminate chain reaction in gas phase by quenching H· and HO· radicals [27, 31]. Secondly, the solid decomposition products of ADP, such as aluminum phosphate, were able to crosslink the decomposition products of RPUF to form compact char layer, which could effectively prohibit mass and heat transmission in combustion area [32, 33].

Thermal stability

TGA was applied to investigate thermal decomposition properties of virgin RPUF and RPUF/ADP composites. TGA and DTG curves in nitrogen atmosphere inert condition at linear heating rate of 20 °C·min^{-1} are shown in Fig. 2. The 5 mass% mass loss temperature ($T_{-5\%}$), the 50 mass% mass loss temperature ($T_{-50\%}$) and the char residue at 700 °C are listed in Table 4. It can be found that the thermal degradation of pure RPUF displayed two-stage process, which was consistent with previous report [34]. The first step occurred in the temperature range of 220–410 °C corresponded to the decomposition of urethane bonds as well as polyol chain segments, with the release of isocyanates, secondary amines, aldehydes, ketones, CO_2, water, et al [35, 36].The second step happened in the temperature of 430–550 °C corresponded to the thermal degradation of isocyanates and aromatic compounds [37]. With the addition of ADP, RPUF/ADP composites presented three-stage process, the

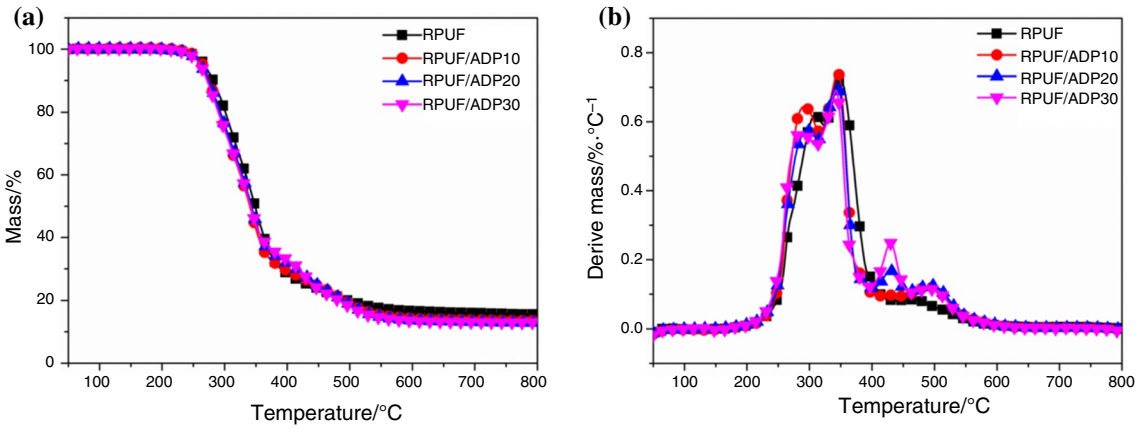

Fig. 2 TGA and DTG curves of RPUF **a** and RPUF/ADP **b** composites in nitrogen atmosphere

Table 4 TG test results of RPUF and PRUF/ADP composites in nitrogen atmosphere

Sample	$T_{-5\%}$/°C	$T_{-50\%}$/°C	T_{max}/°C			Char residue at 700 °C/mass%
			Step I	Step II	Step III	
RPUF	268	348	349	–	466	16.0
RPUF/ADP10	265	340	345	428	487	13.8
RPUF/ADP20	261	342	343	428	493	13.2
RPUF/ADP30	260	341	342	429	492	13.0

new steps at the temperature range of 410–430 °C ascribed to the decomposition of ADP [32]. In addition, pure RPUF presented $T_{-5\%}$ of 268 °C and $T_{-50\%}$ of 348 °C with char residue of 16.0 mass%. Compared with pure RPUF, RPUF/ADP composites showed decreased $T_{-5\%}$ and $T_{-50\%}$ values, indicating the addition of ADP enhanced the early decomposition of RPUF matrix, which may be attributed to Lewis acid–base interactions, attack of phosphinates to polyurethane molecular chain [27, 38]. With regard to the char residue, the value of RPUF/ADP10, RPUF/ADP20 and RPUF/ADP30 was 13.8 mass%, 13.2 mass% and 13.0 mass%, respectively, which may come from the low char residue of ADP in degradation process.

Combustion behavior

Microscale combustion calorimetry (MCC) was an important bench-scale measurement for evaluating the combustion properties of materials and it only needed milligrams of sample [39]. Heat release rate (HRR) curves of RPUF and RPUF/ADP composites are presented in Fig. 3, and the corresponding data are listed in Table 5. As can be observed, pure RPUF presented PHRR value of 202 W g^{-1} with THR value of 25.6 kJ g^{-1}. When 10 php of ADP was added, PHRR value of RPUF/ADP10 was decreased to 193 W g^{-1}. The further increase in ADP loading resulted in significantly decrease in PHRR values for RPUF/ADP

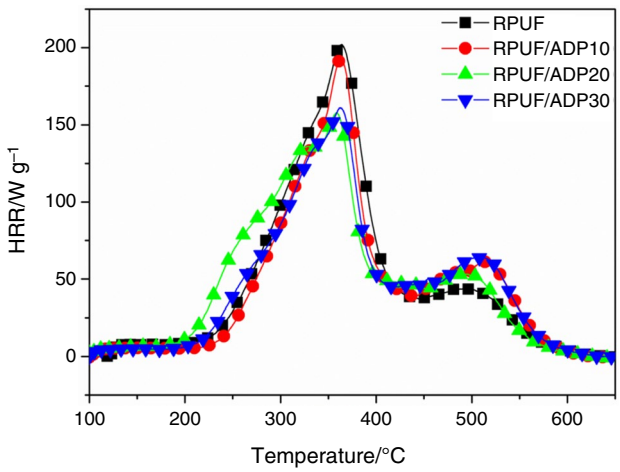

Fig. 3 HRR curves of RPUF and RPUF/ADP composites from MCC test

composites. PHRR value of RPUF/ADP20 was decreased to 158 W g^{-1}, with a reduction of 21.8% compared with RPUF, implying that ADP could significantly decrease PHRR values of RPUF/ADP composites. Moreover, it can be found that the addition of ADP decreased T_{PHRR} values by about 1–5 °C, indicating ADP promoted early degradation of RPUF matrix, which was consistent well with TGA test.

Table 5 MCC results of RPUF and RPUF/ADP composites. (PHRR: Peak of release rate, ± 5 W g^{-1}; THR: Total heat release, ± 0.1 kJ g^{-1}; T_{PHRR}: Temperature at PHRR, ± 2 °C)

Specimen	PHRR/W g^{-1}	THR/KJ g^{-1}	T_{PHRR}/°C
RPUF	202	25.6	364
RPUF/ADP10	193	24.2	363
RPUF/ADP20	158	25.7	359
RPUF/ADP30	161	24.7	362

Volatilized products

Identification of gas products of RPUF and RPUF/ADP composites was investigated by TG–FTIR technology, which could help in understanding the decomposition mechanism of PRUF/ADP composites. The 3D-FTIR spectra of the gas phase in the thermal degradation of RPUF and RPUF/ADP30 were shown in Fig. 4. The peaks around 3700–3800, 3300–3400, 2300–2400, 1500–1800 and 1100–1300 cm^{-1} were noted. Furthermore, FTIR spectra of pyrolysis products at the maximal decomposition rate are presented in Fig. 5. The peaks at 3730 cm^{-1} and 3370 cm^{-1}corresponded to vibration of N–H bond in urethane and O–H bond in water, respectively [40, 41]. The strong peaks at 2310 cm^{-1} and 2360 cm^{-1} confirmed the existence of isocyanate compound and CO_2, which were typical decomposition products of RPUF matrix in first stage. It was also found that the occurrence of peaks at 2930, 2180, 1510, 1260, 1110 cm^{-1} was attributed to hydrocarbons, CO, aromatic compounds and esters.

The typical gaseous products of RPUF/ADP30 were similar to those of RPUF. To make a qualitative contrast, the intensities of typical gas products of RPUF and RPUF/ADP30 were portrayed in Fig. 6. Gram–Schmidt curves showed that RPUF/ADP30 presented higher intensity

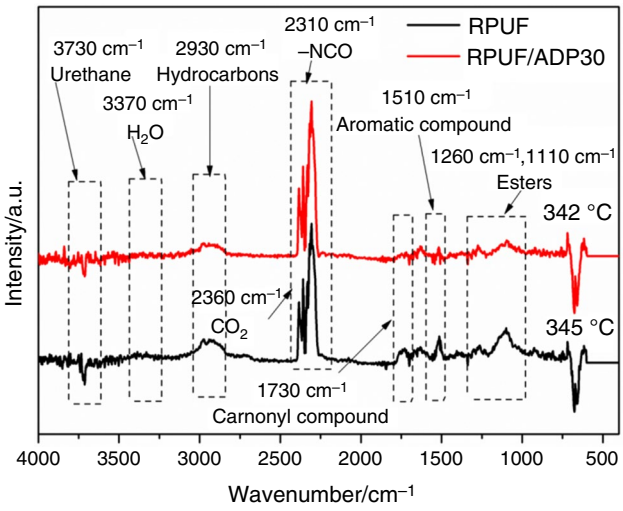

Fig. 5 TG–FTIR spectra of pyrolysis products at maximal decomposition rate of pure RPUF (**a**) and RPUF/ADP30 (**b**)

compared with RPUF in first step, indicating that ADP enhanced early decomposition of RPUF matrix. In addition, RPUF/ADP30 presented higher intensities of CO_2 and isocyanate compound, which was consistent with above mentioned facts. As can be seen in Fig. 6b, RPUF/ADP30 showed lower hydrocarbons intensity compared with that of RPUF, this may come from Lewis acid–base interactions between phosphinates and polyurethane molecular chain, which promoted hydrocarbon segment of polyurethane chain into condensed phase [27]. CO was a typical decomposition product of RPUF mainly released in second stage, which resulted from the pyrolysis of the isocyanates and aromatic compounds. Figure 6e reveals that RPUF/ADP presented lower CO intensity compared with that of RPUF, suggesting ADP inhibited CO release in the second decomposition of RPUF matrix, which was benefit to the people in the fire.

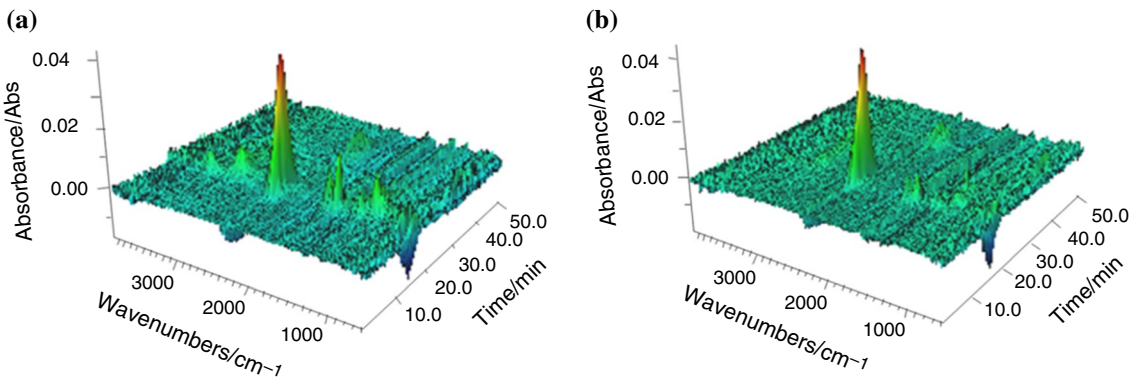

Fig. 4 3D-FTIR spectra of RPUF (**a**) and RPUF/ADP30 (**b**)

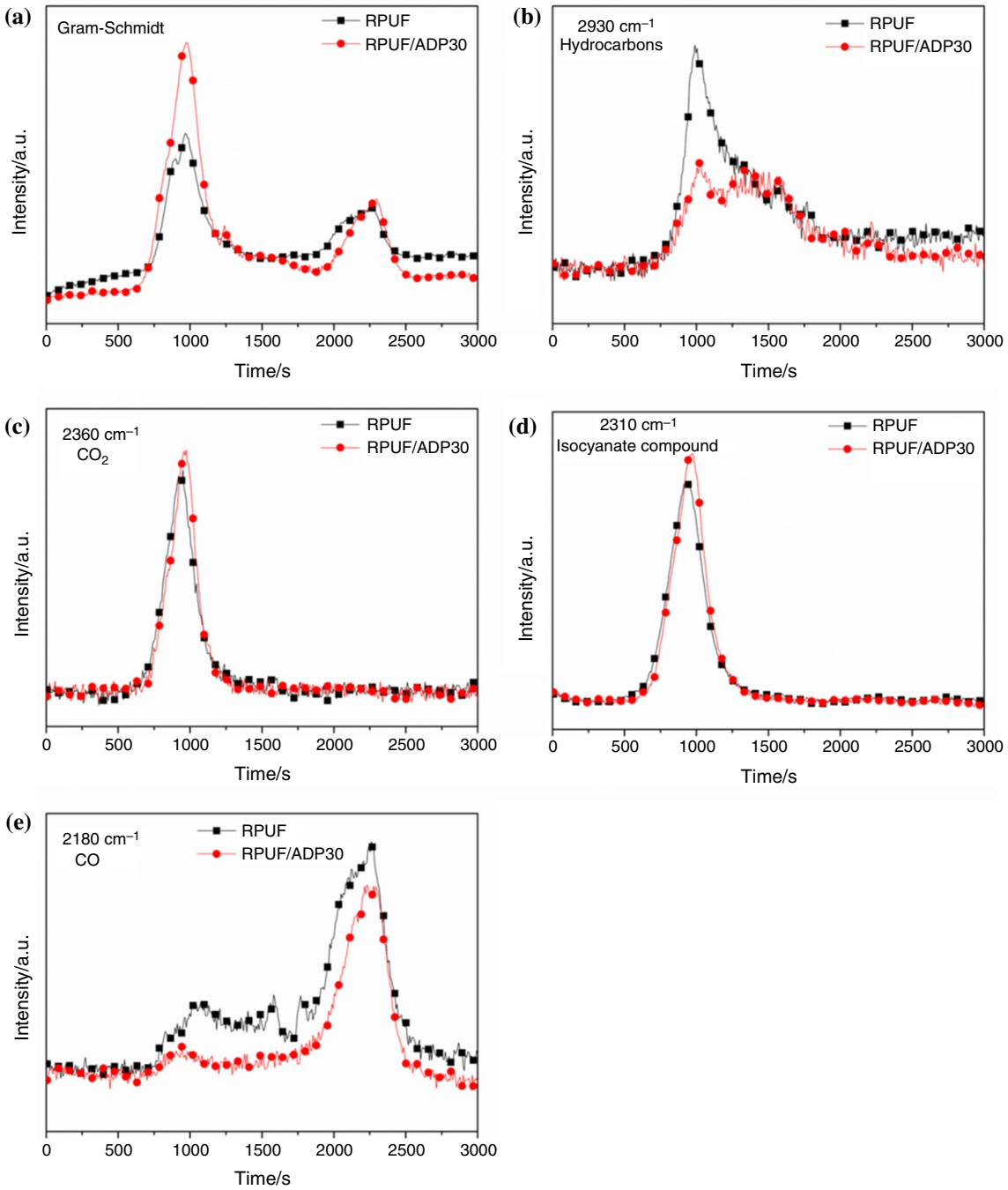

Fig. 6 Absorbance of pyrolysis products of RPUF and RPUF/ADP30 versus time: **a** Gram-schmidt; **b** hydrocarbons; **c** isocyanate compound; **d** CO_2; **e** CO

Char residue analysis

Generally, the char residue of RPUF and RPUF/ADP composites after combustion can give much important information for the flame retardant mechanism. For this reason, the char residue of the samples after calcined in 600 °C for 10 min was collected and characterized by scanning electron microscope. As show in Fig. 7, pure RPUF presented loose char residue with much fragments, which was caused by the gases blow out from inside in the decomposition process of PRUF matrix (Fig. 7a). Such a char cannot effectively inhibit the underlying polyurethane molecular chain from degradation in combustion process. In contrast, RPUF composites with ADP loading showed compact char layer, which served as a barrier to oxygen and flammable gases. The char with this structure could effectively inhibit mass and heat

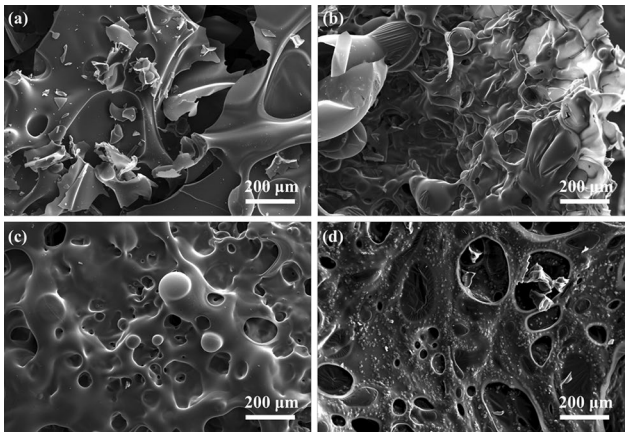

Fig. 7 SEM images of char residue for RPUF and RPUF/ADP composites: **a** RPUF; **b** RPUF/ADP10; **c** RPUF/ADP20; **d** RPUF/ADP30

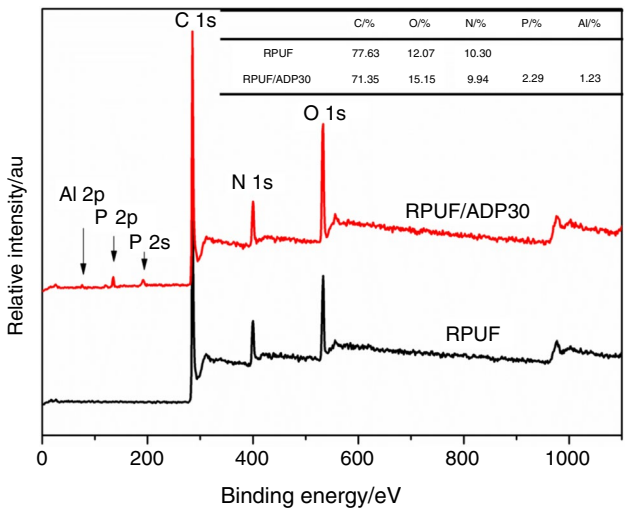

	C/%	O/%	N/%	P/%	Al/%
RPUF	77.63	12.07	10.30		
RPUF/ADP30	71.35	15.15	9.94	2.29	1.23

Fig. 8 XPS spectra of the char residue of RPUF and RPUF/ADP30

transmission and thus significantly retard the burning of the underling materials.

Furthermore, XPS analysis was used to investigate chemical components of char residue for RPUF and RPUF/ADP30, and the corresponding spectra were shown in Fig. 8. The char residue of RPUF contained 77.63% of C, 12.07% of O and 10.30% N, which were come from the polyurethane molecular chain. Char residue of RPUF/30 mainly contained C, O and N, and also few P and Al element which came from ADP. The addition of ADP slightly decreased C and N contents to 71.35% and 9.94%, while increased O content to 15.15%.

To further investigate existing state of C, N and O elements, the peaks were resolved by peak analysis software (XPS PEAK 4.1). Figure 9 presents the bonding state of C element in char residue of RPUF and RPUF/ADP30. The peaks at 284.7 eV can be ascribed to C–H and C–C bond in aliphatic and aromatic species. The bond at around 285.7 eV corresponded to C–O/C–N bond in C–O–C and C–N–C structure. The peaks at 287.4 eV were characteristics of C=O/C=N structure, which may come from carbonyl groups and aromatic heterocyclic structure. The content of the typical bonding state for C element is listed in Table 6. The char residue of RPUF presented C–C/C–H content of 51.38%, C–O/C–N content of 38.89% and C=O/C=N content of 9.73%. The residue of RPUF/ADP30 presented significant increase in C–C/C–H bond content and decrease in C–O/C–N bond content, indicating ADP promoted C element in polyurethane molecular to form stable aromatic structure in combustion, which was benefit for the formation of compact char [42].

Figure 10 shows the bonding state of N element, in which the peak at 400.4 eV was ascribed to N= structure in aromatic heterocyclic, and the peak at 398.7 eV corresponded to –NH–structure. It can be found in Table 6, RPUF/ADP30 presented significantly improved N= structure content,

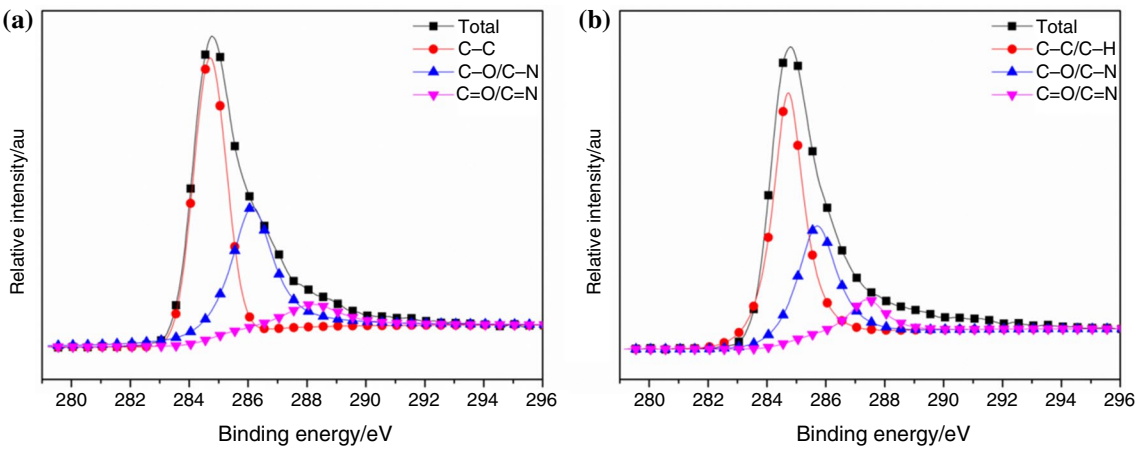

Fig. 9 C1s spectra of char residue of RPUF (**a**) and RPUF/ADP30 (**b**)

Table 6 Bonding state data of C, O, N in char residue of RPUF and RPUF/ADP30

Sample	C			O			N	
	C–C/C–H	C–O/C–N	C=O/C=N	O_2/H_2O	–O–	=O	–NH–	=N
	284.7 eV/%	285.7 eV/%	287.4 eV/%	533.2 eV/%	532.5 eV/%	531.3 eV/%	398.7 eV/%	400.4 eV/%
RPUF	51.38	38.89	9.73	63.98	16.72	19.30	49.06	50.94
RPUF/ADP30	59.60	31.79	8.61	22.24	46.64	31.12	38.05	61.95

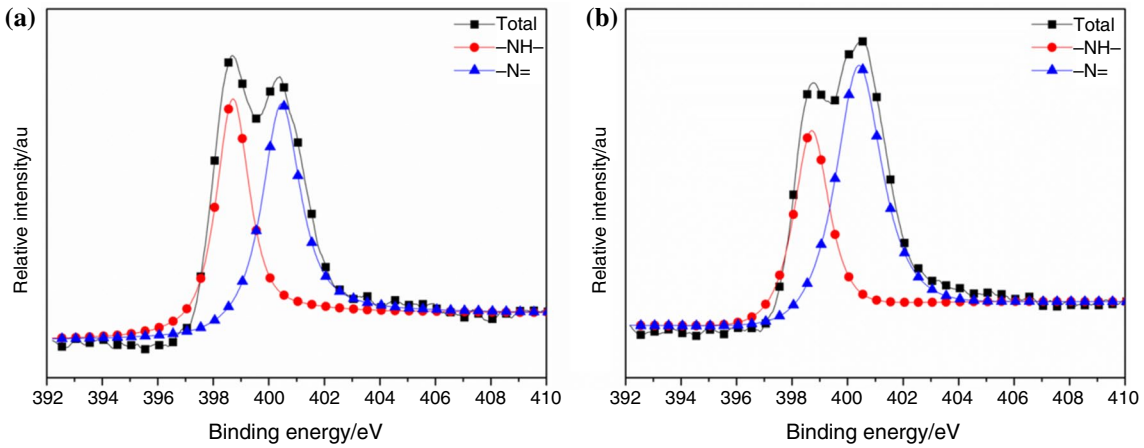

Fig. 10 N1s spectra of char residue of RPUF (**a**) and RPUF/ADP30 (**b**)

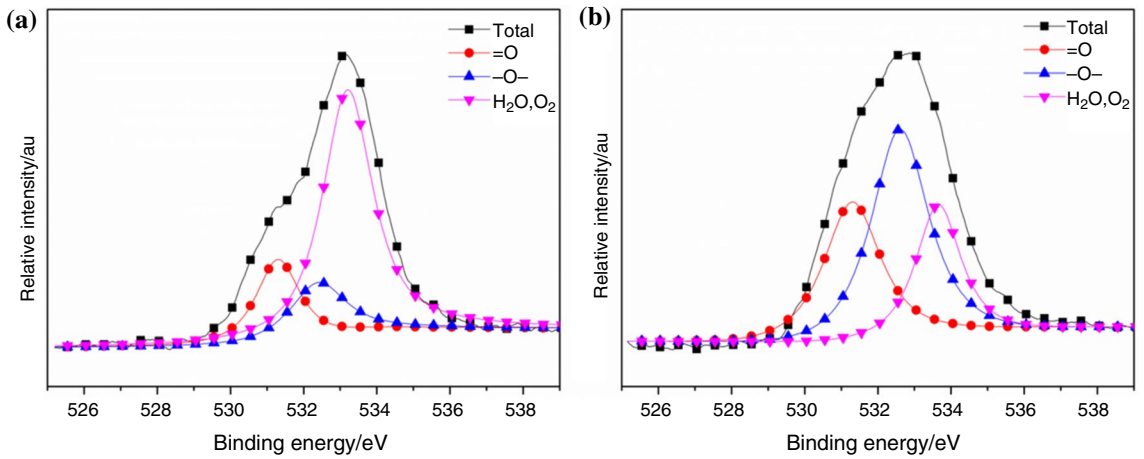

Fig. 11 O1s spectra of char residue of RPUF (**a**) and RPUF/ADP30 (**b**)

indicating ADP can also promote N element to form aromatic heterocyclic structure, which could enhance the compactness of char layer.

Figure 11 displayed the bonding state of O element. The peak at around 533.2 eV was ascribed to the chemisorbed oxygen and absorbed water for the porous structure of the char [43]. The peaks at 532.5 eV confirmed the existence of –O–in C–O–C, C–O–P and C–O–H structure, which can also enhance the compactness of the char. The bond at 531.3 eV corresponded to C=O structure in phosphate and carboxylate. Table 6 showed that the char of RPUF presented high O_2/H_2O content of 63.98%, indicating loose char residue of RPUF, which was consistent well with SEM analysis. In char residue of RPUF/ADP30, the O_2/H_2O content was significantly decreased to 22.24%, confirming the formation

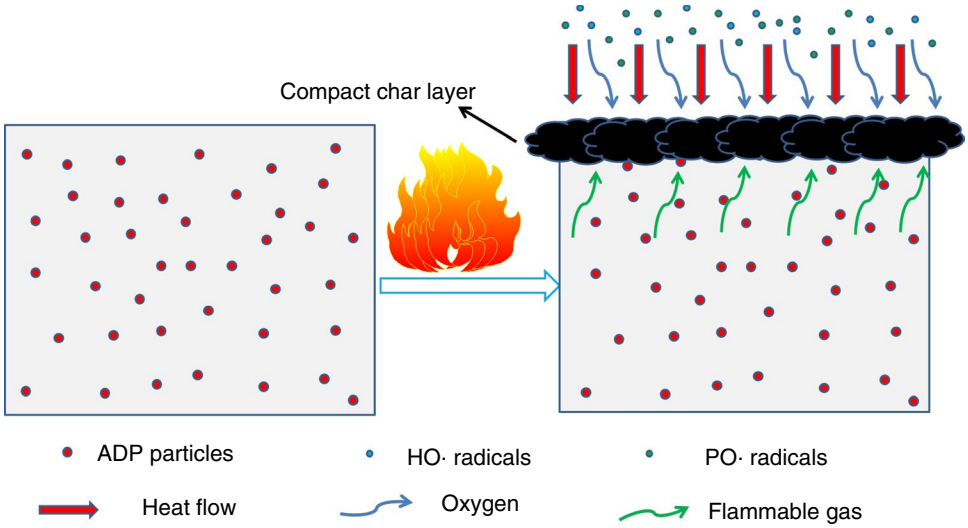

Fig. 12 Schematic illustration for the flame retardancy mechanism of RPUF/ADP composites

of compacted char, which could effectively inhibit mass and heat transmission in combustion.

Mechanism consideration

On the basis on the above datum, the possible mechanism of ADP in RPUF/ADP composites was presented in Fig. 12. ADP could thermal decomposed to oligomers of phosphinates, diethylphosphinic acid and aluminum phosphate [44, 45]. Oligomers of phosphinates and diethylphosphinic acid can further decomposed to P· and PO· radicals in gas phase, which could quench H· and HO· radicals in combustion zone. Furthermore, phosphinate compounds could effectively promote C and N element in polyurethane molecular chain to form aromatic and aromatic heterocyclic structure, which combined with aluminum phosphate to construct compact char layer. The compacted char layer could suppress the mass and heat transfer and effectively retard the burning of the underlying material and significantly enhance flame retardancy of RPUF/ADP composites. Thus, RPUF/ADP composites achieved enhanced fire-resistance property attributed to gas–solid flame retardancy mechanism of ADP.

Conclusions

In this work, RPUF/ADP composites with high flame retardancy were fabricated by one-step water-blown method with the incorporation of ADP. RPUF/ADP composites exhibited enhanced flame retardancy with the loading of ADP. The composites achieved UL-94 V1 rating, a raised LOI value with significant decrease in PHRR value. TG–FTIR test revealed that the incorporation of ADP promoted the release of CO_2, hydrocarbons and isocyanate compound in first stage degradation polyurethane molecular while inhibited the release of CO in second stage degradation. Char residue analysis confirmed that ADP promote C and N element in polyurethane matrix to form aromatic and aromatic heterocyclic structure, enhancing compactness of the char, which could effectively inhibit mass and heat transmission in combustion. All of the above tests indicated that ADP provided a new strategy for preparation of flame retardant RPUF composites.

Acknowledgements This research was supported by National Natural Science Fund of China (Nos. 51403004, 21576001 and U1460106), Open Project of State Key Laboratory Cultivation Base for Nonmetal Composites and Functional Materials (17kffk14), Provincial Natural Science Foundation of Anhui (KJ2016SD08) and Postdoctoral Science Foundation of China (2017M610399).

References

1. Wang X, Hu Y, Song L, Xing WY, Lu HD, Lv P, Jie GX. UV-curable waterborne polyurethane acrylate modified with octavinyl POSS for weatherable coating applications. J Polym Res. 2010;18(4):721–9.
2. Zhang JH, Kong QH, Yang LW, Wang DY. Few layered $Co(OH)_2$ ultrathin nanosheets based polyurethane nanocomposites with reduced fire hazard: from eco-friendly flame retardance to sustainable recycling. Green Chem. 2018;18(10):3066–74.
3. Xu Q, Jin C, Majlingova A, Zachar M, Restas A. Evaluate the flammability of a PU foam with double-scale analysis. J Therm Anal Calorim. 2019. https://doi.org/10.1007/s10973-018-7494-2.
4. Tan CJ, Lee JJL, Ang BC, Andriyana A, Chagnon G, Sukiman MS. Design of polyurethane fibers: relation between the spinning technique and the resulting fiber topology. J Appl Polym Sci. 2019;136(26):47706.
5. Gao L, Zheng G, Zhou Y, Hu L, Feng G. Improved mechanical property, thermal performance, flame retardancy and fire behavior of lignin-based rigid polyurethane foam nanocomposite. J Therm Anal Calorim. 2015;120(2):1311–25.

6. Li LJ, Chen YJ, Qian LJ, Xu B, Xi W. Addition flame-retardant effect of nonreactive phosphonate and expandable graphite in rigid polyurethane foams. J Appl Polym Sci. 2018;135(10):45960.
7. Hejna A, Kosmela P, Kirpluks M, Cabulis U, Klein M, Haponiuk J, Piszczyk Ł. Structure, mechanical, thermal and fire behavior assessments of environmentally friendly crude glycerol-based rigid polyisocyanurate foams. J Polym Environ. 2017;26(5):1854–68.
8. Wang C, Wu YC, Li YC, Shao Q, Yan XR, Han C, Wang Z, Liu Z, Guo ZH. Flame-retardant rigid polyurethane foam with a phosphorus-nitrogen single intumescent flame retardant. Polym Adv Technol. 2017;29(1):668–76.
9. Michałowski S, Pielichowski K. 1,2-Propanediolizobutyl POSS as a co-flame retardant for rigid polyurethane foams. J Therm Anal Calorim. 2018;134(2):1351–8.
10. Luo FB, Wu K, Li DF, Zheng J, Guo HL, Zhao Q, Lu MG. A novel intumescent flame retardant with nanocellulose as charring agent and its flame retardancy in polyurethane foam. Polym Compos. 2015;38(12):2762–70.
11. Liu L, Wang ZZ. High performance nano-zinc amino-tris-(methylenephosphonate) in rigid polyurethane foam with improved mechanical strength, thermal stability and flame retardancy. Polym Degrad Stab. 2018;154:62–72.
12. Wang YT, Wang F, Dong QX, Xie MC, Liu P, Ding YF, Zhang SM, Yang MS, Zheng GQ. Core-shell expandable graphite @ aluminum hydroxide as a flame-retardant for rigid polyurethane foams. Polym Degrad Stab. 2017;146:267–76.
13. Shi XX, Jiang SH, Zhu JY, Li GH, Peng XF. Establishment of a highly efficient flame-retardant system for rigid polyurethane foams based on biphase flame-retardant actions. Rsc Adv. 2018;8:9985–95.
14. Bhoyate S, Ionescu M, Kahol PK, Gupta RK. Castor-oil derived nonhalogenated reactive flame-retardant-based polyurethane foams with significant reduced heat release rate. J Appl Polym Sci. 2018;29(1):47276.
15. Wang SX, Zhao HB, Rao WH, Huang SC, Wang T, Liao W, Wang YZ. Inherently flame-retardant rigid polyurethane foams with excellent thermal insulation and mechanical properties. Polymer. 2018;153:616–25.
16. Li QM, Wang JY, Chen LM, Shi H, Hao JW. Ammonium polyphosphate modified with β-cyclodextrin crosslinking rigid polyurethane foam: enhancing thermal stability and suppressing flame spread. Polym Degrad Stab. 2019;161:166–74.
17. Cao ZJ, Dong X, Fu T, Deng SB, Liao W, Wang YZ. Coated vs. naked red phosphorus: a comparative study on their fire retardancy and smoke suppression for rigid polyurethane foams. Polym Degrad Stab. 2017;136:103–11.
18. Reuter J, Greiner L, Schönberger F, Döring M. Synergistic flame retardant interplay of phosphorus containing flame retardants with aluminum trihydrate depending on the specific surface area in unsaturated polyester resin. J Appl Polym Sci. 2019;136(13):47270.
19. Su DQ, Tang ZH, Xie JF, Bian ZX, Zhang JH, Yang DD, Zhang D, Wang JC, Liu Y, Yuan AH, Kong QH. Co, Mn-LDH nanoneedle arrays grown on Ni foam for high performance supercapacitors. Appl Surf Sci. 2019;469:487–94.
20. Xu JL, Liu XQ, Yang WL, Niu L, Zhao JQ, Ma BX, Kang CH. Influence of montmorillonite on the properties of halogen-antimony flame retardant polypropylene composites. Polym Compos. 2019;40(5):1930–8.
21. Zhang JH, Kong QH, Wang DY. Simultaneously improving the fire safety and mechanical properties of epoxy resin with Fe-CNTs via large-scale preparation. J Mater Chem A. 2018;6(15):6376–86.
22. Kong QH, Wu T, Zhang JH, Wang DY. Simultaneously improving flame retardancy and dynamic mechanical properties of epoxy resin nanocomposites through layered copper phenylphosphate. Compos Sci Technol. 2018;154:136–44.
23. Wang X, Song L, Yang HY, Lu HD, Hu Y. Synergistic effect of graphene on antidripping and fire resistance of intumescent flame retardant poly(butylene succinate) composites. Ind Eng Chem Res. 2011;50(9):5376–83.
24. Zhan Z, Xu M, Li B. Synergistic effects of sepiolite on the flame retardant properties and thermal degradation behaviors of polyamide 66/aluminum diethylphosphinate composites. Polym Degrad Stab. 2015;117:66–74.
25. Wang Y, Zhang L, Yang Y, Cai X. Synergistic flame retardant effects and mechanisms of aluminum diethylphosphinate (AlPi) in combination with aluminum trihydrate (ATH) in UPR. J Therm Anal Calorim. 2016;125(2):839–48.
26. Gu L, Qiu J, Sakai E. Thermal stability and fire behavior of aluminum diethylphosphinate-epoxy resin nanocomposites. J Mater Sci-Mater Electron. 2016;28(1):18–27.
27. Kaya H, Özdemir E, Kaynak C, Hacaloglu J. Effects of nanoparticles on thermal degradation of polylactide/aluminium diethylphosphinate composites. J Anal Appl Pyrolysis. 2016;118:115–22.
28. Thirumal M, Khastgir D, Singha NK, Manjunath BS, Naik YP. Effect of expandable graphite on the properties of intumescent flame-retardant polyurethane foam. J Appl Polym Sci. 2008;110:2586–94.
29. Yang HY, Wang X, Song L, Yu B, Yuan Y, Hu Y, Yuen RKK. Aluminum hypophosphite in combination with expandable graphite as a novel flame retardant system for rigid polyurethane foams. Polym Adv Technol. 2014;25(9):1034–43.
30. Leung SN, Wong A, Wang LC, Park CB. Mechanism of extensional stress-induced cell formation in polymeric foaming processes with the presence of nucleating agents. J Supercrit Fluid. 2012;63:187–98.
31. Braun U, Schartel B, Fichera MA, Jäger C. Flame retardancy mechanisms of aluminium phosphinate in combination with melamine polyphosphate and zinc borate in glass-fibre reinforced polyamide 6,6. Polym Degrad Stab. 2007;92(8):1528–45.
32. Seefeldt H, Duemichen E, Braun U. Flame retardancy of glass fiber reinforced high temperature polyamide by use of aluminum diethylphosphinate: thermal and thermo-oxidative effects. Polym Int. 2013;62(11):1608–16.
33. Zhong L, Zhang KX, Wang X, Chen MJ, Xin F, Liu ZG. Synergistic effects and flame-retardant mechanism of aluminum diethyl phosphinate in combination with melamine polyphosphate and aluminum oxide in epoxy resin. J Therm Anal Calorim. 2018;134(3):1637–46.
34. Camino G, Costa L, Trossarelli L. Study of the mechanism of intumescence in fire retardant polymers: part I-thermal degradation of ammonium polyphosphatepentaerythritol mixtures. Polym Degrad Stab. 1984;6(4):243–52.
35. Chattopadhyay D, Webster DC. Thermal stability and flame retardancy of polyurethanes. Prog Polym Sci. 2009;34(10):1068–133.
36. Yuan Y, Ma C, Shi YQ, Song L, Hu Y, Hu WZ. Highly-efficient reinforcement and flame retardancy of rigid polyurethane foam with phosphorus-containing additive and nitrogen-containing compound. Mater Chem Phys. 2018;211:42–53.
37. Modesti M, Lorenzetti A, Besco S, Hrelja D, Semenzato S, Bertani R, Michelin RA. Synergism between flame retardant and modified layered silicate on thermal stability and fire behaviour of polyurethane nanocomposite foams. Polym Degrad Stab. 2008;93(12):2166–71.
38. Isitman NA, Dogan M, Bayramli E, Kaynak C. The role of nanoparticle geometry in flame retardancy of polylactide nanocomposites containing aluminium phosphinate. Polym Degrad Stab. 2012;97(8):1285–96.
39. Tang G, Wang X, Xing W, Zhang P, Wang BB, Hong NN, Yang W, Hu Y, Song L. Thermal degradation and flame retardance of

biobased polylactide composites based on aluminum hypophosphite. Ind Eng Chem Res. 2012;51(37):12009–16.
40. Wang PS, Chiu WY, Chen LW, Denq BL, Don TM, Chiu YS. Thermal degradation behavior and flammability of polyurethanes blended with poly (bispropoxyphosphazene). Polym Degrad Stab. 1999;66(3):307–15.
41. Yuan Y, Yu BH, Shi YQ, Ma C, Song L, Hu WZ, Hu Y. Highly efficient catalysts for reducing toxic gases generation change with temperature of rigid polyurethane foam nanocomposites: a comparative investigation. Compos Part A Appl Sci. 2018;112:142–54.
42. Tang G, Zhang R, Wang X, Wang BB, Song L, Hu Y, Gong XL. Enhancement of flame retardant performance of bio-based polylactic acid composites with the incorporation of aluminum hypophosphite and expanded graphite. J Macromol Sci A. 2013;50(2):255–69.
43. Wang X, Hu Y, Song L, Xuan SY, Xing WY, Bai ZM, Lu HD. Flame retardancy and thermal degradation of intumescent flame retardant poly(lactic acid)/starch biocomposites. Ind Eng Chem Res. 2011;50(2):713–20.
44. Kaya H, Hacaloglu J. Thermal degradation of polylactide/aluminium diethylphosphinate. J Anal Appl Pyrolysis. 2014;110:155–62.
45. Orhan T, Isitman NA, Hacaloglu J, Kaynak C. Thermal degradation of organophosphorus flame-retardant poly(methyl methacrylate) nanocomposites containing nanoclay and carbon nanotubes. Polym Degrad Stab. 2012;97(3):273–80.